arXiv:1605.03304v1 [astro-ph.GA] 11 May 2016

Significant enhancement of H_2 formation in disk galaxies under strong ram pressure

Benjamin Henderson & Kenji Bekki

ICRAR, M468, The University of Western Australia 35 Stirling Highway, Crawley Western Australia, 6009, Australia

ABSTRACT

We show, for the first time, that H_2 formation on dust grains can be enhanced in disk galaxies under strong ram-pressure (RP). We numerically investigate how the time evolution, of HI and H_2 components in disk galaxies orbiting a group/cluster of galaxies, can be influenced by hydrodynamical interaction between the gaseous components of the galaxies and the hot intra-cluster medium (ICM). We find that compression of HI caused by RP increases H_2 formation in disk galaxies, before RP rapidly strips HI, cutting off the fuel supply and causing a drop in H_2 density. We also find that the level of this H_2 formation enhancement in a disk galaxy under RP depends on the mass of its host cluster dark matter (DM) halo, initial positions and velocities of the disk galaxy, and disk inclination angle with respect to the orbital plane. We demonstrate that dust growth is a key factor in the evolution of the HI and H_2mass in disk galaxies under strong RP. We discuss how the correlation between H_2 fractions and surface gas densities of disk galaxies evolves with time in the galaxies under RP. We also discuss whether or not galaxy-wide star formation rates (SFRs) in cluster disk galaxies can be enhanced by RP if the SFRs depend on H_2 densities.

Subject headings: galaxies: evolution — galaxies: ISM — galaxies: star formation — galaxies: structure — galaxies: clusters: intracluster medium

1. Introduction

It is well known that galaxy environments play key roles in morphological transformation of galaxies, enhancement and quenching of galaxy-wide star formation, and cold gas evolution of galaxies (e.g., Dressler 1980; Koopmann & Kenny 2004; Boselli & Gavazzi 2006; Bundy et al. 2010; Villalobos et al. 2014; Pasquali 2015; Cortese et al. 2016). Dynamical and hydrodynamical interactions influence galaxy evolution (e.g., Bekki 2009; Bekki & Couch

2011), mergers and intracluster medium (ICM) affect fundamental galactic parameters with increasing likelihood in higher density regions (e.g., Lambas et al. 2012). Star forming regions peak in merging systems in small and compact groups, increasing SFRs and having important effects on galaxy morphology and evolution. Hydrodynamical interactions between ICM and cold interstellar medium (ISM) of disk galaxies aid in the quenching of star formation (SF), and hence, reddening of galaxies through 'strangulation' (e.g., Peng et al. 2015).

Ram-pressure stripping (RPS) has long been considered to be one of the most important environmental effects and thus has been investigated by many observational and theoretical astronomers (e.g., Gunn & Gott 1972; Takeda et al. 1984; Vollmer et al. 2001; Kronberger et al. 2008; Book & Benson 2010; Bekki 2014; McPartland et al. 2016). These studies include disk gas stripping (e.g., Roediger & Hensler 2005), halo gas stripping (e.g., Bekki 2009), stripped gas tails (e.g., Irwin et al. 1987; Tonnesen & Bryan 2012) and cold gas compression (e.g., Ebeling et al. 2014). The compression of cold gas initially induces SF in the galaxy, while the stripping of the disk and halo gas causes an eventual decrease in SF in the galaxy. RP is an essential physical process that controls SF histories and gas evolution in disk galaxies.

These previous studies have not extensively investigated how RP of ICM in group and cluster environments can influence the evolution of HI and H_2 components of disk galaxies. Yagi et al. (2013) showed that SF occurs in the stripped tails from galaxies under RP, stripping of H_2 from a disk galaxy would cause faster SF-quenching in the galaxy as it is the direct fuel in the SF process. HI stripping only aids in the eventual 'strangulation' of the galaxy and is a more long term effect on the galaxy evolution. Compression of the H_2 left in the disk galaxy induces SF due to an increase in density and interactions of H_2. Further work into the RP effect on H_2 is necessary to understand the formation and evolution of the cold gas in disk galaxies within group and cluster environments.

The purpose of this letter is to show, for the first time, that strong RP can significantly enhance H_2 formation on dust grains in disk galaxies based on the results of numerical simulations. We also show how this enhancement of H_2 formation depends on model parameters such as orbits within groups/clusters and disk inclination angles with respect to their orbital planes. Since H_2 is the key parameter in the formation of giant molecular clouds (GMCs) and thus star formation, we discuss the present new results in the context of galaxy-wide H_2 formation and star formation within dense galaxy environments. In the present work, we do not discuss the origin of the shock-excited H_2 in disk galaxies, which has been recently discovered by Wong et al. (2014), because the present simulation code does not allow us to investigate H_2 formation through gaseous shocks.

2. The model

To investigate time evolution of HI and H_2 content of disk galaxies under ram pressure of ICM, we use our original chemodynamical simulation code that can be run on GPU machines (Bekki 2013, B13). This new code enables us to investigate time evolution of dust and formation of H_2 on the surface of dust grains in a fully self-consistent manner, though does not include feedback effects of active galactic nuclei (AGNs). The most important difference between the present study and previous ones (e.g., Christensen et al. 2012 ; Hopkins et al. 2014) is the self-consistent time evolution of dust abundances deriving H2 abundances used in the present study, whereas others used constant dust-to-metal ratios (i.e., no evolution of dust abundances). In the present study, a disk galaxy moves in a cluster with a halo dark matter (DM) mass, $M_{\rm dm}$, and an ICM temperature, $T_{\rm ICM}$, allowing its cold gas to be influenced by RP of the ICM. The RP force is calculated according to the position and velocity of the galaxy with respect to the cluster centre (for details see Bekki 2014, B14).

The disk galaxy is composed of dark matter halo, stellar disk, stellar bulge and gaseous disk, similar to the Milky Way (MW-type). The total masses of dark matter halo, stellar disk, gas disk, and bulge are set to be $10^{12}M_{\odot}$, $6\times10^{10}M_{\odot}$, $6\times10^{9}M_{\odot}$ and $10^{10}M_{\odot}$, respectively. The mass ratio of dark matter halo to disk is fixed at 16.7. We adopt the density distribution of the NFW halo (Navarro, Frenk & White 1996) suggested from CDM simulations, with c-parameter and virial radius set to 10 and 245 kpc, respectively. The spherical bulge is represented by the Hernquist model with scale length of 0.7 kpc and size of 3.5 kpc. The radial (R) and vertical (Z) density profiles of the stellar disk are assumed to be proportional to $\exp(-R/R_0)$ with scale length $R_0 = 0.2R_{\rm s}$ and to $\mathrm{sech}^2(Z/Z_0)$ with scale length $Z_0 = 0.04R_{\rm s}$, respectively. The gas disk, where $R_{\rm g} = 2R_{\rm s}$, has radial and vertical scale lengths of $0.2R_{\rm g}$ and $0.02R_{\rm g}$, respectively. In the present MW-type models the exponential disk has $R_{\rm s} = 17.5$ kpc and $R_{\rm g} = 35$ kpc and a Toomre's parameter of $Q = 1.5$. Star formation, chemical evolution, and dust evolution are included in exactly the same way as in B13. The total number of particle used in the MW-type model is 1033400, with gravitational softening length of 2.1 kpc and 200 pc for the disk dark and baryonic components, respectively. The maximum hydrogen density in the present simulation is $\sim 8\times10^3$ cm^{-3}, which is significantly lower than H_2 density of molecular clouds (MCs) cores ($\sim 10^5$ cm^{-3}). This lack of resolution for MCs cores will not be a problem in this study, because we focus exclusively on galaxy-scale H_2 distribution.

To avoid a large number of gas particles to represent the entire ICM (e.g., Abadi et al. 1999), it is represented by 60^3 SPH particles in a cube with the size of $R_{\rm ICM}$ and a disk galaxy is placed in the exact centre. The initial velocity of each SPH particle for the ICM is set to be ($V_{\rm r}(t=0)$, 0, 0), where $V_{\rm r}$ is determined by the position of the galaxy with respect

to the cluster centre. The orbit direction is chosen as the x-axis and disk inclination angles θ and ϕ are defined with respect to the x-y plane of the ICM cube. θ is the angle between the spin axis of the disk and the z-axis (i.e., $\theta = 0$ means the spin axis parallel to the z-axis), whereas ϕ is the angle between the x-y projected spin axis and the x-axis.

The mass of ICM particle is time-dependent and calculated according to the mass density of ICM at the position of the galaxy at each time step whereas $T_{\rm ICM}$ is assumed to be constant. The ICM is assumed to have a uniform distribution within the cube with $R_{\rm ICM}$ set to be $6R_{\rm s}$ and $T_{\rm ICM}$ set to be 5.6×10^6K and 2.6×10^7 K for $M_{\rm h} = 10^{13} M_\odot$ and $M_{\rm h} = 10^{14} M_\odot$, respectively; $T_{\rm ICM}$ is much higher than the temperature of cold ISM in galaxies. We include periodic boundary conditions (at $R_{\rm ICM}$) for the ICM SPH particles leaving the cube. We mainly described the results of 10 representative models in the present study, because these models show typical behaviours of H_2 evolution in disks under strong RP and intriguing parameter dependence, see Table 1 for model parameter values.

3. Results

Figure 1 shows how RP influences the time evolution of HI and H_2 masses and spatial distributions in a disk galaxy for five models (M1-M5). In the mass distributions of model M1, it can be seen that gas is first strongly compressed and then stripped efficiently form the galaxy. At $T = 1.41$ Gyr, just before peri-centre passage, the cold gas has clumped together with small amounts stripped. The majority of the stripping can in fact be seen at $T = 1.76$ Gyr, corresponding to the galaxy leaving the cluster central region. This indicates that the gas in the disk galaxy first undergoes compression (a shallower decrease in HI mass) and is then stripped (a steeper decrease in HI mass). Compression of the HI can enhance HI density significantly, particularly in the central region, and thus drives efficient formation of H_2 on dust grains in the disk galaxy. As a results, H_2 mass can significantly increase with a peak occurring at the peri-centre passage. H_2 mass begins to decrease after this through stripping of gas and formation of new stars from H_2. The initial decrease of H_2 mass at $T < 0.5$ Gyr is due to the rapid gas consumption by SF.

As shown in Figure 1, RP effects on H_2 differ slightly for the five models (M1-M5) with different disk inclination angles (θ and ϕ). Although H_2 formation enhancement can be seen in all of these models, the level of this enhancement depends weakly on θ and ϕ. The more edge-on models (M1, M2 and M5) have a higher rate of H_2 loss, through H_2 stripping and star formation (driven by compression of H_2). This indicates H_2 formation efficiency on dust grains in disks under RP depends on the inclination of the disk to the orbital plane of the galaxy. The models M1 and M5 have higher gas mass loss and RP effects on the disk galaxy

than the edge-on model M2, which is an interesting result suggesting there is a unique angle where RP has most effect. However, this is beyond the scope of this letter and we will discuss the origin of this further in future papers.

Figure 2 describes how the correlation between gas surface density ($\Sigma_{\rm g}$) and H_2 fraction can change with time in the disk galaxy under RP for the fiducial model M1. In the early phase of disk galaxy evolution ($T = 0.35$ Gyr), the galaxy shows a weak positive correlation between $\Sigma_{\rm g}$ and $f_{\rm H_2}$ for $\Sigma_{\rm g} \leq 10\ M_\odot\ {\rm pc}^{-2}$. There is an increase in H_2 gas fraction between $T = 0.35$ Gyr and $T = 1.41$ Gyr in local gaseous regions, indicating H_2 formation is enhanced in these local regions of the galaxy. There is little stripping of gas between $T = 0.35$ and 1.41 Gyr, as overall surface gas density does not change so significantly. Stripping of gas is evident between $T = 1.41$ Gyr and $T = 1.76$ Gyr by the large drop in the overall surface gas density. These results are consistent with and reinforce what is shown in Figure 1. The move to low mean surface gas density and high H_2 fraction in individual gaseous regions of the disk galaxy at $T = 2.47$ Gyr is indicative of HI being stripped throughout the galaxy and not just the outer disk. The almost horizontal line of average H_2 fraction indicates that HI and H_2 are confined to the same pixels (i.e., the same local regions) within the disk galaxy.

Figure 3 demonstrates how different galaxy orbits within clusters of galaxies and different cluster masses ($M_{\rm dm}$) influence time evolution of HI and H_2 mass in disk galaxies. The peak of H_2 mass still corresponds to the peri-centre passages of galaxies in these models (M6-M9). Model M6 has a shallower orbit than M1-M5, due to a higher initial galactic velocity, causing less RP to influence the disk galaxy and less gas to be stripped. H_2 mass peaks in this model significantly shallower than models with smaller peri-centre distances (M1-M5). Similarly to models M1-M5 in Figure 1, the most prominent stripping occurs as the galaxy leaves the cluster central region. Model M7, with lower $M_{\rm dm}$ (group-like halo) and an effective tighter orbit of the galaxy, produces more rapid stripping of HI (steep slope in HI mass) resulting in less H_2 formation (low H_2 mass peak) than other models (M1-M5). This is likely due to the disk galaxy spending more time in the most central region of the group where ICM is higher density. Contrast to this, model M8 has a wide orbit never passing the most central region of the cluster. There is little RPS of HI and no peak in H_2 mass, as HI is not being compressed and not driving formation of H_2. Model M9, with a very close orbit (due to an initial position closer to the cluster centre) and a lower $M_{\rm dm}$ (group-like halo), has two peri-centre passes during $\sim$2.8 Gyr. HI is rapidly stripped due to the galaxy being in the cluster central region and H_2 is formed and stripped during the first peri-centre passage. During the second passage little increase in H_2 mass is seen, as there is insufficient HI to compress and form copious amounts of H_2.

Figure 4 shows how dust growth can influence time evolution of H_2 and SF histories

in disk galaxies under RP. H_2 mass in the model M10 without dust physics is considerably lower with only a slight peak at the peri-centre pass. This indicates that little H_2 formation is occurring in the disk galaxy for this model (M10). Owing to consumption of gas and dust by star formation, H_2 formation on dust grains cannot continue to be effective without dust mass increase through accretion of gas-phase metals onto dust grains (i.e., dust growth). It is interesting to note that appreciable enhancement of galaxy-wide star formation can be seen in these two models with and without dust physics. This SF enhancement cannot last long owing to H_2 consumption by star formation and gas stripping during and after peri-centre passage. These results imply that dust physics needs to be included in modelling of H_2 evolution of disk galaxies under RP.

4. Discussion and conclusions

Formation and evolution of H_2 in galaxies is a fundamental process in understanding star formation and evolution of cold gas in disk galaxies. We have shown how formation of H_2 is influenced through HI compression associated with RP of a disk galaxy in the present study. As the disk galaxy undergoes RP effects H_2 mass in the galaxy increases, due to enhanced H_2 formation efficiency — higher density of compressed gas can significantly enhance the conversion from HI to H_2 on dust grains. The present simulations does not have sub-pc resolution so that the evolution of H_2 in molecular clouds of disk galaxies under RPS cannot be investigated. Using 3D MHD simulations of H_2 formation within molecular clouds, Valdivia et al. (2015) have already investigated (i) how H_2 formation in dense molecular clouds occurs rapidly and (ii) how H_2 then spreads into more defuse regions around the clouds. It is our future work to investigate how RP can influence H_2 formation and evolution within individual molecular clouds in disk galaxy using more sophisticated high-resolution 3D MHD simulations.

The present study has shown that there exists a weak positive correlation between H_2 gas fraction (f_{H_2}) and surface gas density (Σ_g) in disk galaxies under RP when HI is being compressed (yet not stripped). This result is consistent with observational studies for disk galaxies in the Virgo cluster (Nakanishi et al. 2006), which have revealed a similar $f_{H_2} - \Sigma_g$ relation in NGC4254 and NGC4656 (See Figure 3 of Nakanishi et al. 2006). These two galaxies are further from the cluster centre and are concluded by Nakanishi et al. (2006) as to have not yet been stripped of HI. The other three galaxies in their paper (NGC4402, NGC4569 and NGC4579) are stripped of HI and the gas fraction and surface density are consistent with our findings after strong RPS. So far only a few observational studies have investigated a $f_{H_2} - \Sigma_g$ relation of disk galaxies in cluster environments. Future observations

of HI and H_2 of disk galaxies in clusters will allow us to discuss the possible influence of RP on H_2 formation and evolution in disk galaxies under RP.

The present study has revealed that the evolution of H_2 in disk galaxies under RP depends strongly on their orbits, disk inclination angles, and cluster/group masses ($M_{\rm dm}$). For example, models with a more edge-on disk galaxy orientation show more efficient H_2 formation by compression from RP. Also, in a lower DM mass cluster halo, the disk galaxy is required to have a closer orbit to the cluster centre for RP to be effective, as more time needs to be spent in higher density ICM region. These results imply that SFHs of these galaxies can be significantly influenced by these parameters, because galaxy-wide SFRs can be determined by H_2 densities. McPartland et al. (2016) have recently discussed how a galaxy falling into a cluster at high velocities causes an extreme RPS event and gives rise to the 'jellyfish' morphology classification (Ebeling et al. 2014) and would possibly have higher fractions of H_2 gas.

H_2 formation from gaseous phase HI is unlikely to occur, as gas particles simply cannot release enough energy when they encounter one another (e.g., Gould & Salpeter 1963; Valdivia et al. 2015). The most commonly accepted solution is for H_2 to form on the surface of dust grains in the ISM (e.g., Gould & Salpeter 1963; Duley & Williams 1993; Le Bourlot et al. 2012). Here we have shown, for the first time, that dust growth is crucial in rapid enhancement of H_2 formation on dust grains in disk galaxies under RP. This implies that large-scale (group/cluster-scale) hydrodynamical effects can influence very small-scale physics of H_2 formation on dust grains. This also implies that dust evolution can control the evolution of HI and H_2 content of disk galaxies in groups/clusters. Almost all previous galaxy-scale and cosmological-scale simulations of galaxy formation and evolution in these dense environments did not include dust physics (e.g., Bekki 2013), and accordingly their predictions on cold gas content would not be so robust. It is thus our future study to understand better the important roles of dust in evolution of cold gas of group/cluster galaxies using cosmological simulations with more sophisticated models of dust evolution.

We are grateful to the anonymous referee for constructive and useful comments.

REFERENCES

Abadi, M. G., Moore, B., & Bower, R. G. 1999, MNRAS, 308, 947

Bekki, K. 2009, MNRAS, 399, 2221

Bekki, K., & Couch, W. J. 2011, MNRAS, 415, 1783

Bekki, K. 2013, MNRAS, 432, 2298 B13

Bekki, K. 2014, MNRAS, 483, 444 B14

Book, L. G., & Benson, A. J. 2010, ApJ, 716, 810

Boselli, A., & Gavazzi, G. 2006, PASP, 118, 517

Bundy, K., Scarlata, C., Carollo, C. M., et al. 2010, ApJ, 719, 1969

Christensen, C., Quinn, T., Governato, F., et al. 2012, MNRAS, 425, 3058

Cortese, L., Bekki, K., Boselli, A., et al. 2016, arXiv:1604.01505 (accepted in MNRAS)

Ebeling, H., Stephenson, L. N., & Edge, A. C. 2014, ApJL, 781, L40

Dressler, A. 1980, ApJ, 236, 351

Duley, W. W¿, & Williams, D. A. 1993, MNRAS, 260, 37

Gould, R. J., & Salpeter, E. E. 1963, ApJ, 138, 393

Gunn, J. E., & Gott, J. R, III 1972, ApJ, 176, 1

Hopkins, P. F., Kereš, D., Oñorbe, J., et al. 2014, MNRAS, 445, 581

Irwin, J. A., Seaquist, E. R., Taylor, A. R., & Duric, N. 1987, ApJL, 313, L91

Koopmann, R. A., & Kenney, J. D. P. 2004, ApJ, 613, 851

Kronberger, T., Kapferer, W., Unterguggenberger, S., Schindler, S., & Ziegler, B. L. 2008, A&A, 483, 783

Lambas, D. G, Alonso, S., Mesa, V., & O'Mill, A. L. 2012, A&A, 539, A45

Le Bourlot, J., Le Petit, F., Pinto, C., Roueff, E., & Roy, F. 2012, A&A, 541, A76

McPartland, C., Ebeling, H., Roediger, E., & Blumenthal, K. 2016, MNRAS, 455, 2994

Nakanishi, H., Kuno, N., Sofue, Y., et al. 2006, ApJ, 651, 804

Navarro, J. F., Frenk, C. S., & White, S. D. M. 1996, ApJ, 462, 563

Pasquali, A. 2015, Astronomische Nachrichten, 336, 505

Peng, Y., Maiolino, R., & Cochrane, R. 2015, NAT, 521, 192

Roediger, E., & Hensler, G. 2005, A&A, 433, 875

Takeda, H., Nulsen, P. E. J., & Fabian, A. C. 1984, MNRAS, 208, 261

Tonnesen, S., & Bryan, G. L. 2012, MNRAS, 422, 1609

Valdivia, V., Hennebelle, P., Gerin, M., & Lesaffre, P. 2015, arXiv:1512.03979

Villalobos, Á., De Lucia, G., & Murante, G. 2014, MNRAS, 444, 313

Vollmer, B., Cayatte, V., Balkowski, C., & Duschl, W. J. 2001, ApJ, 561, 708

Wong, O. I., Kenney, J. D. P., Murphy, E. J., & Helou, G. 2014, ApJ, 783, 109

Yagi, M., Gu, L., Fujita, Y., et al. 2013, ApJ, 778, 91

This preprint was prepared with the AAS LaTeX macros v5.2.

Table 1. Description of parameter values for the ten representative models.

Model ID [a]	$M_{\rm dm}$ [b]	$X_{\rm g}$ [c]	$Y_{\rm g}$ [d]	$V_{\rm g}$ [e]	θ [f]	ϕ [g]	Dust growth [h]
M1	1.0	0.5	0.5	0.3	45	30	Yes
M2	1.0	0.5	0.5	0.3	0	0	Yes
M3	1.0	0.5	0.5	0.3	90	0	Yes
M4	1.0	0.5	0.5	0.3	60	30	Yes
M5	1.0	0.5	0.5	0.3	30	0	Yes
M6	1.0	0.5	0.5	0.5	45	30	Yes
M7	0.1	0.5	0.5	0.3	45	30	Yes
M8	1.0	1.0	1.0	0.3	45	30	Yes
M9	0.1	0.3	0.3	0.3	45	30	Yes
M10	1.0	0.5	0.5	0.3	45	30	No

[a]The fiducial model is M1.

[b]The initial group/cluster dark matter halo mass in units of $10^{14} M_{\odot}$.

[c]The initial x-position in units of $r_{\rm vir}$, where $r_{\rm vir}$ is the virial radius of the group/cluster.

[d]The initial y-position in units of $r_{\rm vir}$, where $r_{\rm vir}$ is the virial radius of the group/cluster.

[e]The initial x-component of the velocity in units of $v_{\rm c}$, where $v_{\rm c}$ is the circular velocity at the position.

[f]The initial inclination angle θ of a disk galaxy.

[g]The initial inclination angle ϕ of a disk galaxy.

[h]'Yes' ('No') means dust growth and destruction are (not) included in the model.

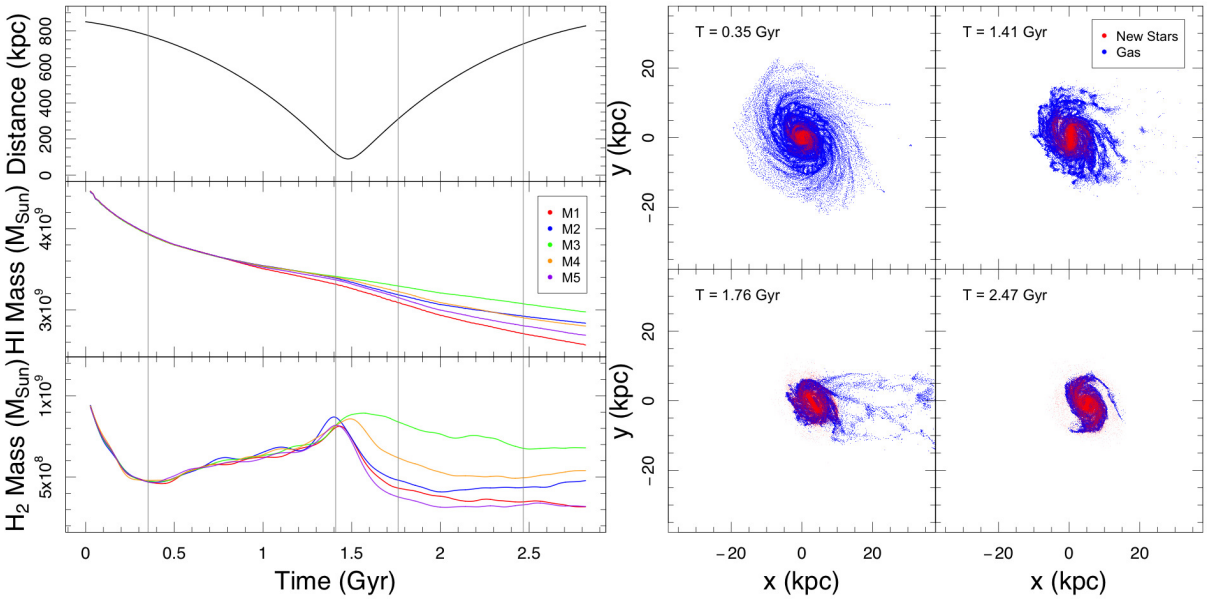

Fig. 1.— Left is the galaxy orbit (top), HI mass (middle) and the H_2 mass (bottom) over ∼2.8 Gyr evolution of disks for the models M1, M2, M3, M4 and M5 (red, blue, green, orange and purple respectively). The orbit is represented as the distance of the galaxy to the centre of the cluster in kpc. H_2 and HI mass are measured in solar masses. Right is the positions (in units of kpc) of the new star and gas particles (red and blue respectively), for model M1, projected onto the x-y plane showing four time steps ($T = 0.35$ Gyr, $T = 1.41$ Gyr, $T = 1.76$ Gyr, and $T = 2.47$ Gyr), indicated on the left by vertical grey lines.

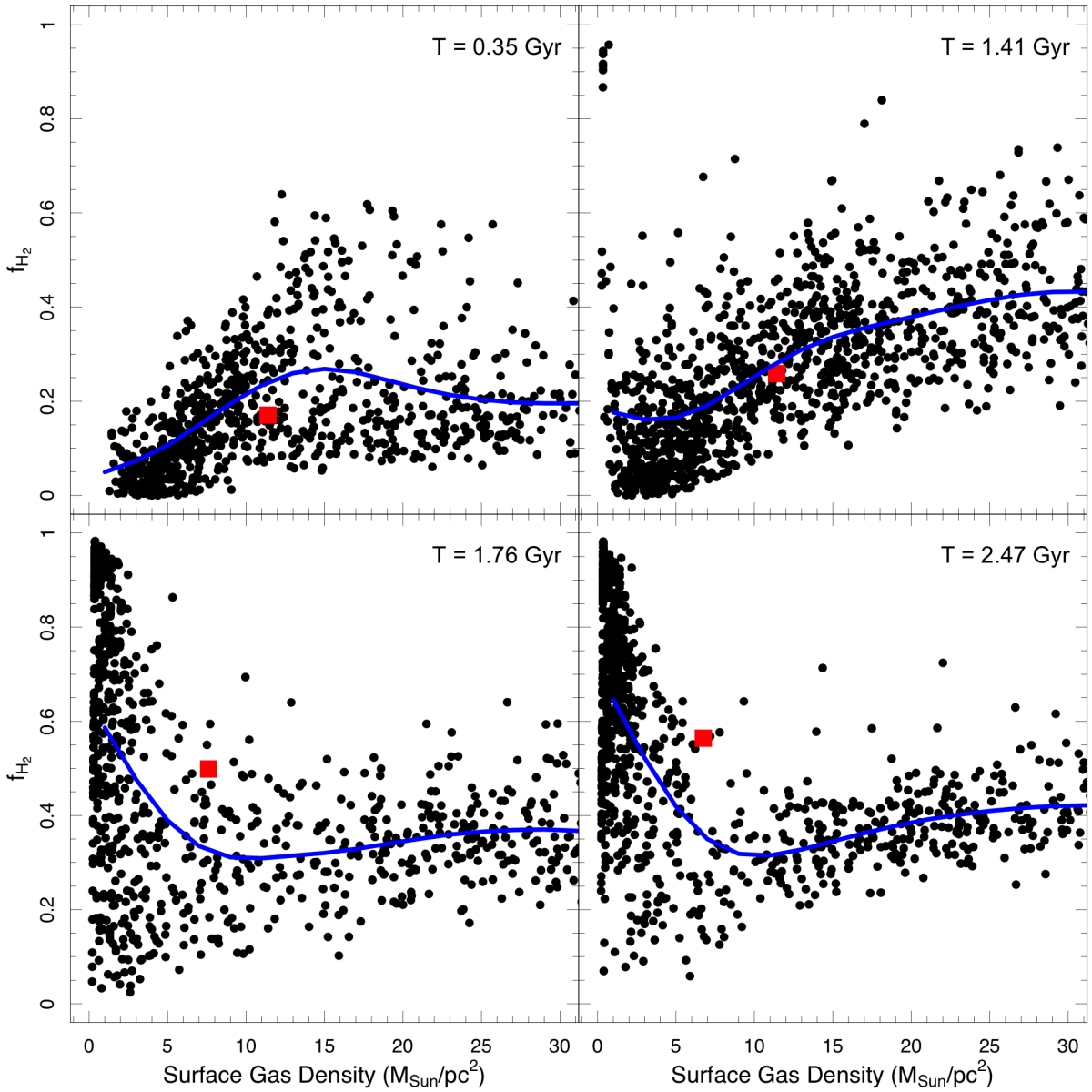

Fig. 2.— H_2 gas fraction and surface gas density are determined for a 50 by 50 grid points in the x-y plane for model M1, 25 kpc^2 from the centre. Points represent values for one grid point. H_2 gas fraction is H_2 mass over HI mass and surface density is total gas mass over the area of the pixel in units of $M_\odot$/pc^2. The red squares are the average gas fraction and the average surface density, and the blue lines are the average gas fraction over the surface density. Four time steps are shown: $T = 0.35$ Gyr (top left), $T = 1.41$ Gyr (top right), $T = 1.76$ Gyr (bottom left), and $T = 2.47$ Gyr (bottom right).

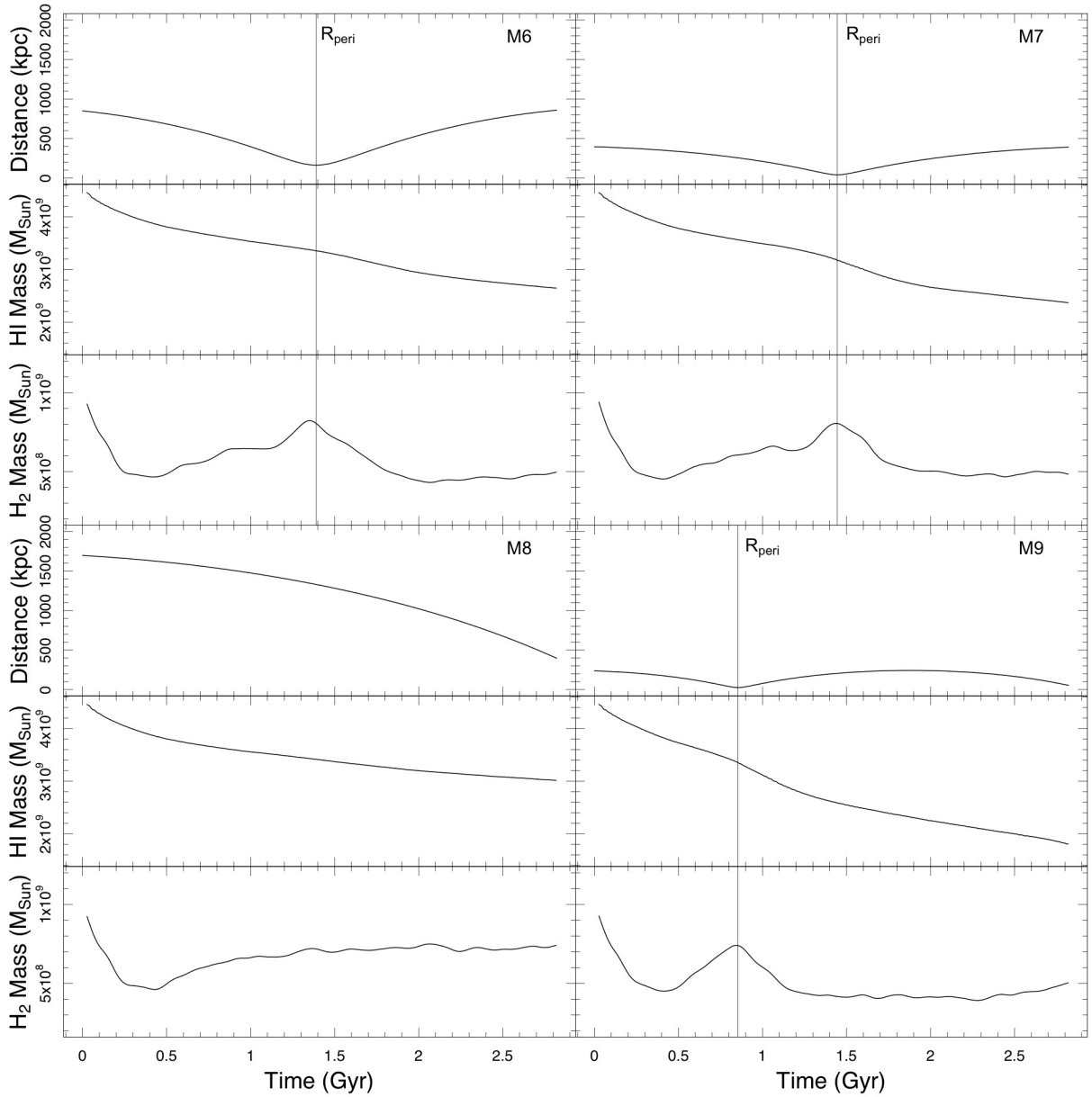

Fig. 3.— Galactic orbit and HI and H_2 mass for the models: M6 (top left), M7 (top right), M8 (bottom left) and M9 (bottom right). The orbit of the galaxy is represented as cluster-centric distance in kpc and H_2 and HI mass are in units of $M_\odot$. The vertical line represents the galaxy's peri-centre passage (R_{peri}) of the cluster.

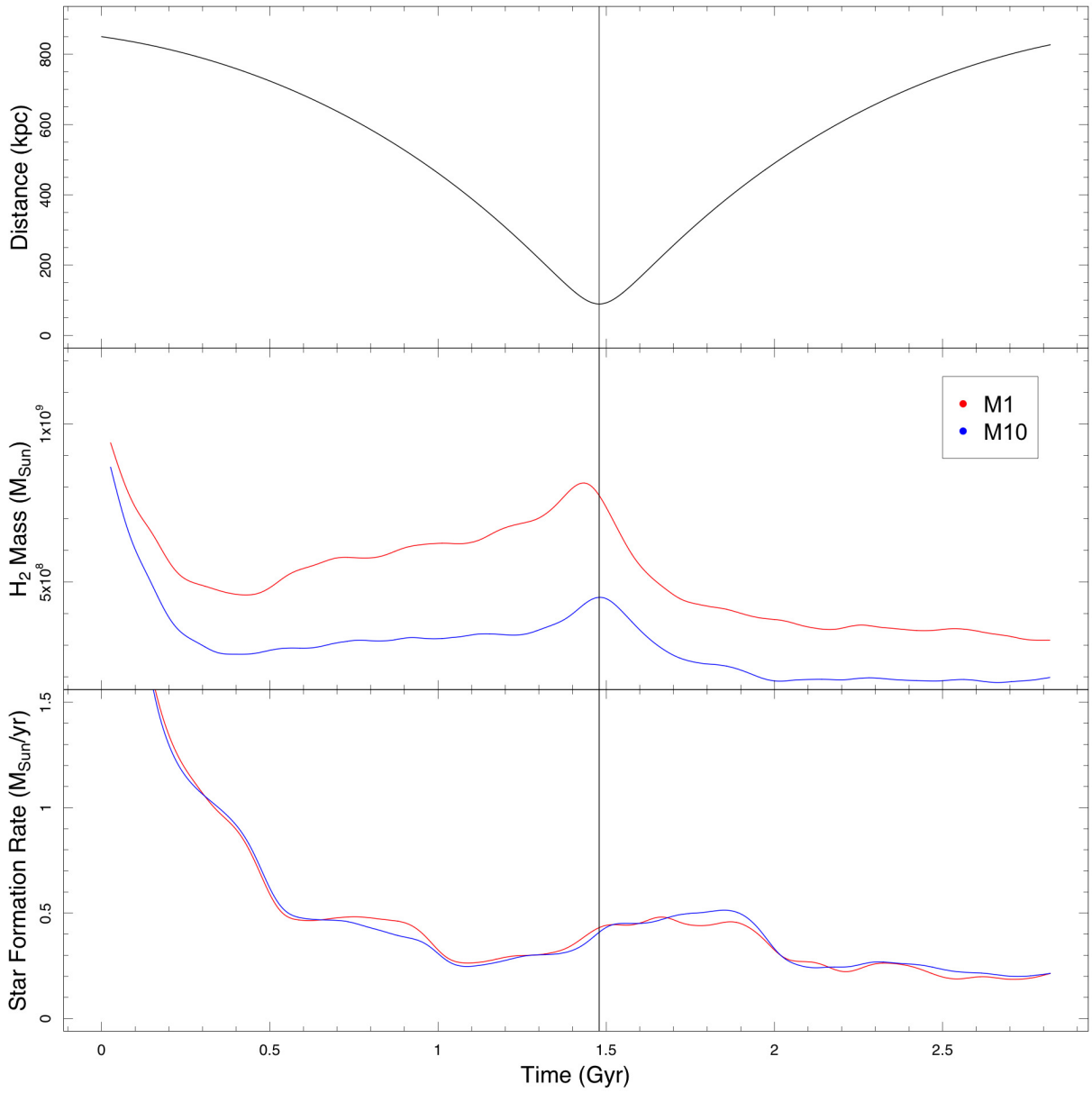

Fig. 4.— The galactic orbit (top), H_2 mass (middle) and the SFR (bottom) are shown for model M1 (red) and model M10 (blue). As in Figures 1 and 3, orbit is represented as cluster-centric distance in kpc, H_2 mass is in units of $M_\odot$ and SFR is in units of $M_\odot$/yr.